Optical limiting with semiconductors

E. W. Van Stryland, Y. Y. Wu, D. J. Hagan, M. J. Soileau, and Kamjou Mansour

Center for Research in Electro-Optics and Lasers, University of Central Florida, Orlando, Florida 32816

Received February 1, 1988; accepted March 11, 1988

We present a detailed characterization of the output of passive semiconductor-based optical limiters. These devices utilize two-photon absorption along with photogenerated carrier defocusing within the material to limit the output fluence and irradiance. In addition to protecting downstream optical components, the focusing geometry combined with these nonlinearities makes the devices self-protecting. Such devices have a broad working wavelength range since both the initial two-photon absorption and the subsequent carrier refraction are slowly varying funtions of wavelength. For example, ZnSe should have a useful range of from 0.5 to 0.85 μm. In this material we have observed the onset of limiting at input powers as low as 80 W when using 10-nsec, 0.53 μm input pulses. At the same wavelength, when 30 psec pulses into a monolithic ZnSe limiter are used, limiting begins at $\simeq$300 W or 10 nJ. We also monitored the output spatial energy distribution along with the temporal response at each position, using a 2-psec-resolution streak camera. We found that the output fluence along with the output irradiance is effectively limited below detector damage thresholds over an input range of 4 orders of magnitude. Additionally, since both two-photon absorption and the associated self-defocusing increase with decreasing band-gap energy, similar devices using narrow-gap semiconductors should have considerably lower limiting thresholds.

1. INTRODUCTION

Passive optical limiting results from irradiance-dependent nonlinear-optical processes in materials.[1,2] The ideal optical limiter has the characteristics shown in Fig. 1. It has a high linear transmission for low input (e.g., energy E or power P), a variable limiting input E or P, and a large dynamic range defined as the ratio of E or P at which the device damages (irreversibly) to the limiting input. Since a primary application of the optical limiter is for sensor protection, and damage to detectors is almost always determined by fluence or irradiance, these are the quantities of interest for the output of the limiter. Getting the response of Fig. 1 turns out to be possible by using a wide variety of materials; however, it is difficult to get the limiting threshold as low as is often required and at the same time to have a large dynamic range. Because high transmission for low inputs is desired, we must have low linear absorption. These criteria lead to the use of two-photon absorption and nonlinear refraction. In this paper we present the detailed operational characteristics and a theoretical description of optical limiting devices based on two-photon absorption and the subsequent photogenerated free-carrier defocusing in semiconductors. Such devices can be made to have low limiting thresholds, large dynamic ranges, and broad spectral responses. For example, a monolithic ZnSe device limits at inputs as low as 10 nJ (300 W) and has a dynamic range greater than 10^4 for 0.53-μm, 30-psec (FWHM) pulses. Also, the input–output characteristics of this device should not change significantly for input wavelengths from 0.5 to 0.85 μm. While the devices demonstrated operate in the visible, we give theoretical arguments why considerably lower limiting thresholds should be obtainable in the infrared by using narrow-band-gap semiconductors.

2. BACKGROUND

Irradiance-dependent phenomena related to optical limiting were observed first in liquids.[3,4] In 1964 Leite *et al.* used self-action (nonlinear refraction) as a means to measure low absorption in liquids.[5] In 1966 Reickhoff reported irradiance-dependent self-defocusing in liquids.[6] One year later Leite *et al.* demonstrated an optical limiter that used thermal blooming in nitrobenzene and, along with a spatial filter, regulated the output power of a cw Ar laser to 30 mW.[7]

In 1980 CS_2 was tested as a limiting medium.[8] The experiments, using a focused geometry similar to that of Leite *et al.* but with nanosecond pulses, showed that the mechanisms that limit the transmission of this device are self-focusing and absorption associated with the resulting laser-induced breakdown.[8,9] An apparent advantage of liquid-based limiters is that they self-heal, permitting high dynamic ranges limited only by damage to cell windows. The response time has been shown to be 2 psec in the visible.[10] Even larger nonlinearities were found at 10 μm when CO_2 pulses were used, which demonstrates the potential of extremely broadband operation.[11] Additionally, the limiting power can be varied by adjusting the concentration of CS_2 in solvents. However, the critical power P_c is often too high for many applications (e.g., $P_c \simeq 8$ kW at 0.5 μm) and can only be raised, not lowered, by mixing CS_2 with solvents.

Large refractive nonlinearities (several orders of magnitude higher than that of CS_2) have been found in liquid crystals; however, this occurs at the expense of speed (response times are usually nanoseconds or longer).[12–14] When picosecond pulses were used in a comparative study of limiting in seven liquid crystals, Soileau *et al.* found that two-photon absorption was responsible for the limiting behavior.[15]

Atomic vapors have also been used to build optical limiters. Bjorkholm *et al.* built a device that uses the self-focusing in Na vapor that is due to near-resonant excitation at a wavelength of 590 nm.[16] This device also exhibited optical bistability.

Some of the largest nonlinearies exhibited to date are in semiconductors.[17] Unfortunately, from the standpoint of optical limiting, these extremely large nonlinearities are associated with near-band-gap resonance and thus are in a

0740-3224/88/091980-10$02.00

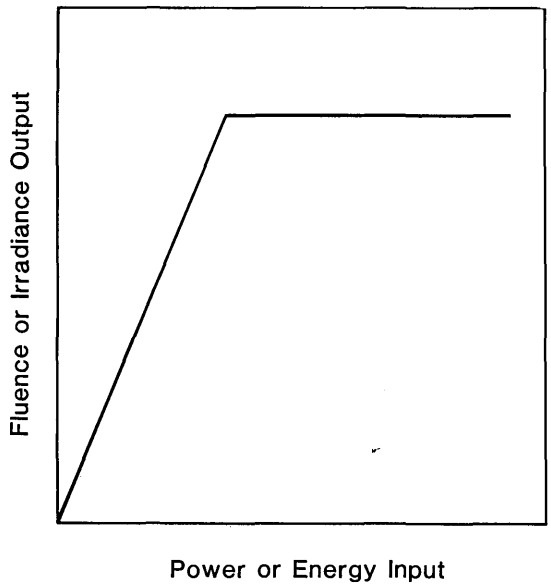

Fig. 1. Fluence or irradiance output of an ideal optical limiter as a function of the input power or energy.

region of relatively high linear absorption. In addition, solids undergo irreversible optical damage. Even so, effective limiting has been demonstrated by using other mechanisms. In 1969 Geusic *et al.* reported limiting behavior in Si attributed to stepwise nonlinear absorption with 1.06-μm radiation.[18] Later Boggess *et al.* showed fluence limiting in Si that was due to a combination of nonlinear absorption with a refractive contribution induced by the photoexcitation of free carriers.[19] Power-limiting experiments were conducted by Ralston and Chang in a series of semiconductors such as CdS, GaAs, and CdSe.[20] This was the first report to our knowledge of the use of two-photon absorption (2PA) for optical limiting. In those studies nanosecond pulses were used when absorption by the 2PA-generated free carriers was significant. In addition, although this was not noted at the time, the refractive-index change caused by the photogenerated carriers was strong and also useful in the limiting process. In particular, this defocusing limits the transmitted fluence. Another type of limiter, which uses the combination of 2PA and nonlinear refraction at 10 μm, was developed by Walker *et al.*[21] This device relies on the étalon properties of the nonlinear sample, and the device also exhibits regions of bistability.[22] While this device has the advantage of not requiring a spatial filter (i.e., it is a true power limiter as opposed to a fluence limiter), the range of input energies over which limiting is obtained is small. Boggess *et al.* were the first to use the combined effects of 2PA and carrier defocusing to obtain optical fluence limiting.[23] The geometry used was to focus picosecond 1.06-μm pulses onto the surface of a thin sample of GaAs, refocus the beam, and monitor the transmission of an aperture. Since the damage-prone surfaces are subjected to the maximum fluence of the input pulses, the range over which these devices function without incurring damage is low. What we have found is that, if thick samples are used, the large nonlinearities of the semiconductor can actually be used to prevent damage.[24] The trick is simply to focus the light tightly into the bulk of the material. Nonlinear absorption combined with nonlinear refraction keeps the irradiance within the semiconductor below the damage threshold, and the device is self-protecting. One problem now is that the wave equation can no longer be separated into two propagation equations, one for the irradiance and one for the phase. This makes even numerical solutions difficult. However, we find that the analysis of thin limiters qualitatively describes the operation of thick limiters.

We recently used this combination of nonlinearities to build optical limiters for the visible based on ZnSe and ZnS.[24] These limiters work exceedingly well for picosecond inputs for which carrier absorption is negligible while carrier defocusing is still strong.[25] Figure 2 shows the geometrical arrangement of a monolithic optical limiter. The device acts as a unity-power inverting lens for low inputs. For high inputs the beam is depleted by 2PA and is defocused following the path shown schematically by the dashed lines in Fig. 2. Figure 3 shows the output fluence detected through an aperture as a function of the input energy of 30-psec, 0.53-μm pulses. The laser used in the picosecond experiments is a passively mode-locked Nd:YAG laser with a single pulse switched out. Residual linear absorption of $\simeq$0.4 cm^{-1} in the chemical-vapor-deposited ZnSe causes the linear transmission at low inputs to be $\simeq$30%. The limiting begins at $\simeq$10-nJ input, which corresponds to $\simeq$300 W. Note the change of scale in Fig. 3. If the original scale were continued, and the ordinate were 7.6 cm, the page would have to be extended for nearly 6 m. The slope shown is indeed extremely small. The device was tested up to a few hundred

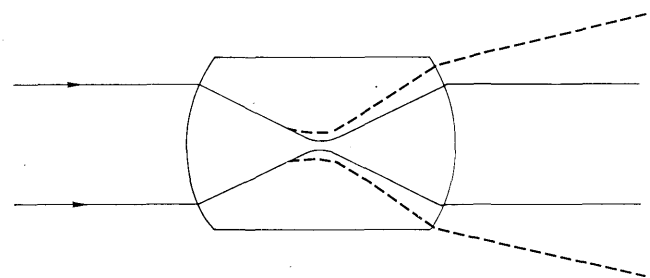

Fig. 2. Schematic of the monolithic optical limiter showing optical paths for low (solid lines) and high (dashed lines) inputs.

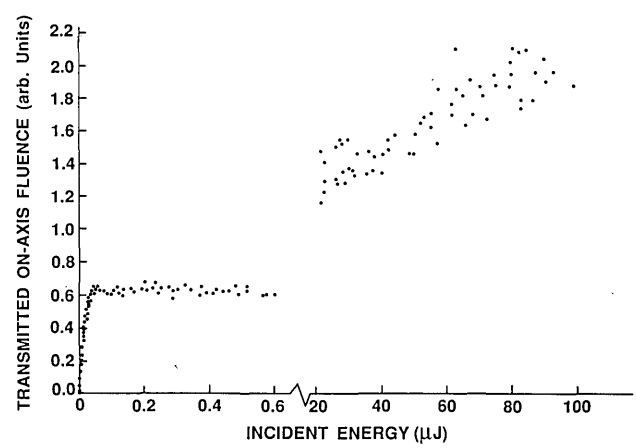

Fig. 3. Plot of the output of a monolithic ZnSe limiter (interpreted as the on-axis fluence detected through an aperture) as a function of the input energy of 30-psec FWHM, 0.53-μm pulses.

microjoules input, demonstrating a dynamic range of greater than 10^4. However, the device was not tested to destruction, and it should withstand pulses of a few millijoules input. In what follows we describe in greater detail the operation of this device, its limitations, and possible extension to other wavelengths by using the results of a fundamental study of 2PA and self-refraction in several semiconductors.

3. MECHANISMS

As will be seen, the primary limiting mechanism is two-photon-induced free-carrier refraction. In earlier research we measured the 2PA coefficients, β, of 10 different semiconductors. These experiments were performed on thin samples (1–5-mm thickness), using collimated $\simeq$1-mm beam-radius picosecond pulses. In this geometry self-refraction is external, the sample acts as a thin lens, and the transverse Laplacian can be neglected in the wave equation for propagation within the nonlinear material.[26] This permits separation of the wave equation into the following equations:

$$\frac{dI}{dz} = -\alpha I - \beta I^2 \tag{1}$$

and

$$\frac{d\Phi}{dz} = -\gamma N = \frac{2\pi}{\lambda}\Delta n, \tag{2}$$

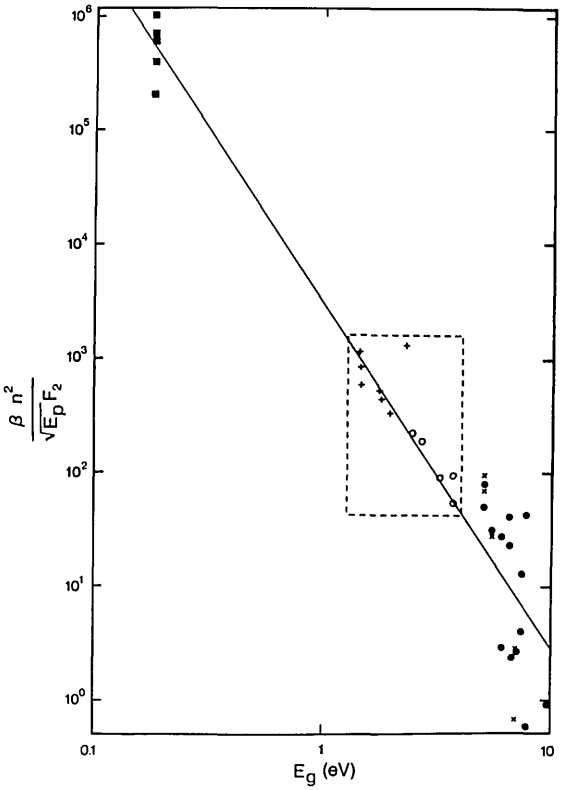

Fig. 4. Logarithmic plot of the scaled 2PA coefficient β as a function of the band-gap energy E_g (in electron volts). E_p is nearly material independent ($\simeq$21 eV), F_2 is a function of the ratio $2\hbar\omega/E_g$, and n is the refractive index. The straight line is a fit to the data within the dashed box for a line of fixed slope −3. The data to the right of the box are taken from Ref. 28 using the third (×) and fourth (●) harmonics of 1.06-μm picosecond pulses. The data to the left of the box are taken from Ref. 29 using 10-μm nanosecond pulses, which carefully accounted for free-carrier absorption.

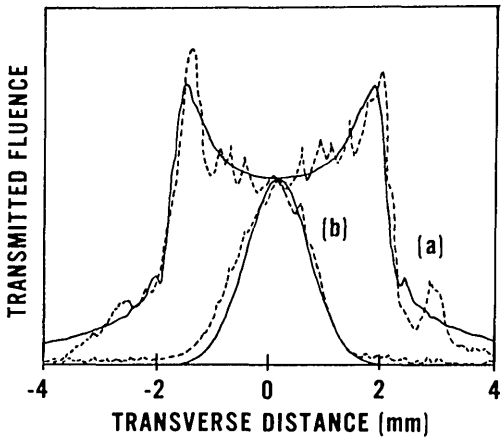

Fig. 5. Vidicon scan of 92-psec FWHM 1.06-μm pulses of spot radius w_0 = 1.0 mm transmitted through a 2-mm-thick sample of CdSe and viewed at a distance of 0.5 m behind the sample. The dashed lines are for (a) 1 GW/cm^2 and (b) 30 MW/cm^2. The solid lines are theoretical fits for the defocusing per carrier. This figure is reproduced from Ref. 30.

where I is the irradiance, α is the linear absorption coefficient, Φ is the slowly varying phase of the field, γ is the Drude contribution to the index change including band blocking, Δn is the change in refractive index, and N is the density of two-photon-generated free carriers.[2] The equation governing the carrier generation, with $\hbar\omega$ the photon energy, is

$$\frac{dN}{dt} = \frac{\beta I^2}{2\hbar\omega}. \tag{3}$$

In writing Eqs. (1)–(3) we have made use of the fact that for picosecond pulses free-carrier absorption can be neglected, as we experimentally verified.[27] We also verified in four-wave mixing experiments that recombination and diffusion of free carriers can be ignored within the 30-psec pulse width. Nonlinear refraction [Eq. (2)], observed in free-space propagation experiments, was entirely explained by carrier defocusing. This last observation allowed us to neglect bound electronic self-focusing. Carefully collecting all the transmitted energy on large-area uniform-response detectors in the very near field allowed us to use Eq. (1) and to measure the 2PA coefficients directly. Using measurements of β for 10 semiconductors, we verified that

$$\beta \propto \sqrt{E_p}\,\frac{F_2\left(\frac{2\hbar\omega}{E_g}\right)}{n^2 E_g^{\,3}}, \tag{4}$$

where n is the linear refractive index and E_p is related to the transition matrix element and is nearly material independent.[27] The function F_2, as calculated for two simple parabolic bands, is given by

$$F_2(x) = (x-1)^{3/2}/x^5. \tag{5}$$

The constant of proportionality in relation (4) found in these experiments is $(3.1 \pm 0.5) \times 10^3$, where E_g and E_p are in electron volts and β is given in centimeters per gigawatt. Using these results, we can predict 2PA coefficients for other materials at other wavelengths as shown in Fig. 4, given only n, E_p, E_g, and $\hbar\omega$. Figure 4 is a log–log plot of the data shown to emphasize the primary dependence of β on E_g. Our data

are enclosed within the dashed box. The solid line has a slope of −3 and best fits the data within the box. It is extended to higher and lower values of E_g to permit us to predict β for other materials. Toward higher values of E_g we are no longer looking at semiconductors but at insulators (e.g., ADP, KDP, and SiO_2).[28] The fact that even here β is given, in most cases, to within better than a factor of 4 is quite remarkable. Toward the left, however, there are few available data except for InSb at 10 μm.[29] The line goes through the center of mass of these points even though this is nearly a 4-orders-of-magnitude extrapolation of β.

In addition to 2PA, defocusing caused by the 2PA-generated carriers was measured by monitoring the free-space propagation in the near field.[30] Figure 5, taken from Ref. 30, shows the normalized near-field spatial energy distribution for low- and high-input irradiance picosecond 1.06-μm pulses transmitted through a 2-mm-thick CdSe sample and propagated a distance of 0.5 m. The solid lines show a single parameter fit for the defocusing produced per carrier [γ in Eq. (2)] given the 2PA-generation rate [Eq. (3)] as measured in Ref. 27 and shown in Fig. 4. This defocusing agrees with Drude theory, including interband blocking [see Eq. (7) in Section 6 below].

4. APPLICATION TO LIMITING

Looking at Fig. 5, we see the fluence-limiting possibilities of a semiconductor-based limiter. Not only will 2PA deplete the transmitted beam but carrier defocusing spreads the beam in space, thus reducing the energy density. Such limiting using thin samples has been demonstrated by detecting the energy transmitted through an aperture after free-space propagation.[23] Limiters used in this thin-sample external self-refraction geometry have been extensively analyzed by Hermann *et al.*[31,32] The limitation of such devices is their low dynamic range. Since the light is focused onto the sample in order to get a low limiting threshold, the fluence is high on the damage-prone surface, and irreversible damage occurs within 1 or 2 orders of magnitude of limiting.[23] A method to alleviate this problem is to use thick samples (thickness larger than the depth of focus) and to focus into the bulk of the material, reducing the irradiance on the damage-prone surface. We find that this geometry, shown in Fig. 6, gives something extra. Not only is the irradiance reduced on the surface but for high inputs the 2PA and defocusing reduce the irradiance in the bulk, preventing damage. This happens while a low limiting threshold is maintained. Unfortunately, Eqs. (1) and (2) are no longer valid, and a quantitative description is difficult. What happens can be qualitatively described as follows.

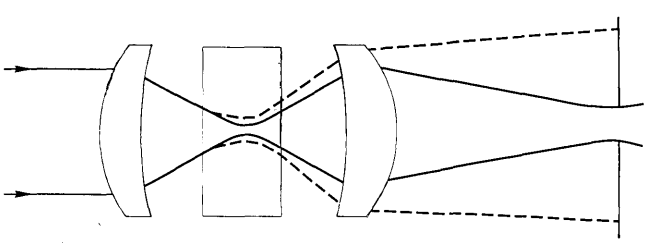

Fig. 6. Schematic drawing of the thick limiter geometry. The solid lines show linear beam propagation for low inputs, and the dashed lines show the beam for high inputs.

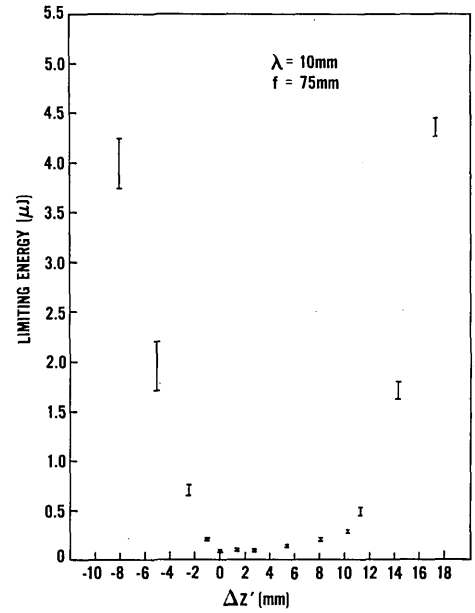

Fig. 7. Plot of the limiting energy E_L as a function of the distance behind the front surface of a 1-cm-thick slab of ZnSe to the linear focal position. The pulse width is 30 psec FWHM, and the beam size at the 7.5-cm focal-length lens is 0.9 mm.

At low inputs, the thick limiter acts linearly, as does the thin limiter. For inputs near the thin limiter's threshold, the thick limiter behaves linearly except in a region near the focal position as determined by linear optics. Only in this region (within the focal volume) does the irradiance become high enough to have significant 2PA along with subsequent carrier defocusing. Thus it is not surprising that the threshold remains constant to within a factor of 2–3 as the position of focus within the thick limiter is varied. This is shown experimentally in Fig. 7, where the limiting threshold is plotted as a function of the position of the linear focus with respect to the front surface of a 1-cm-thick ZnSe slab.[25] At higher inputs the irradiance becomes large enough to have significant 2PA well in front of the linear focal position. This has two consequences. First, the beam at focus will be depleted, making it more difficult to damage. Second, and more importantly, the negative phase change induced on the wave front by the photogenerated carriers negates the beam convergence before focus. The beam is defocused, and damaging irradiances are never reached within the material. The dynamic range is now limited only by front-surface damage. In principle this threshold can be made arbitrarily high by making the optics larger.

Figure 8 shows the output of a thick limiter device using an aperture placed $\simeq$30 cm behind the second lens. The limiting is only weakly dependent on the focal length of the second lens and the distance to the aperture. Also shown is the limiting effect of 2PA by itself when all the transmitted energy is collected. The primary limiting mechanism (fluence limiting, as shown in Fig. 8) is seen to be defocusing. Using limiters in this configuration with picosecond 0.5-μm pulses and tight focusing, we have obtained limiting energies down to $\simeq$14 nJ, corresponding to a peak power of $\simeq$400 W, with a dynamic range of $\simeq 10^3$. With nanosecond pulses the limiting power is actually reduced. This is true because for a fixed irradiance longer pulses create more free carriers, as

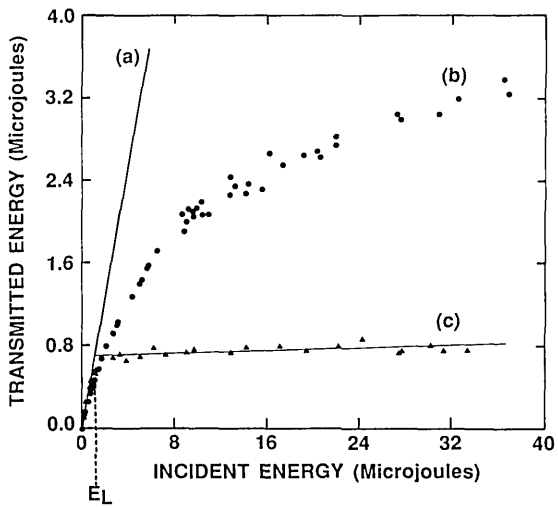

Fig. 8. Input/output characteristics of a ZnSe thick optical limiter showing (a) the linear transmission, (b) the effects of two-photon absorption (i.e., all energy collected), (c) a plot of the transmitted energy through an aperture (i.e., fluence in arbitrary units) as a function of the input 0.53-μm picosecond pulses.

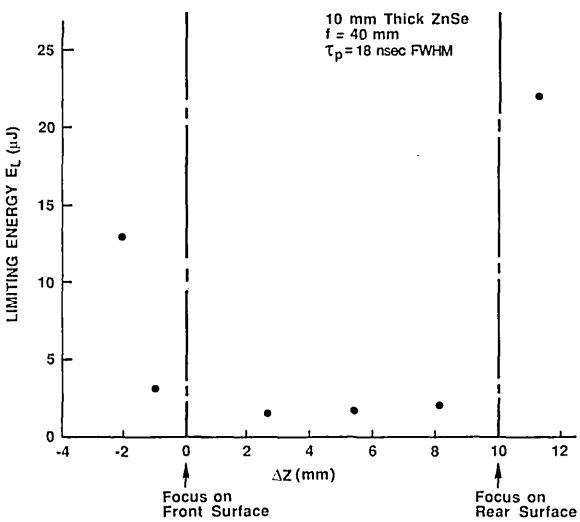

Fig. 9. Plot of the limiting energy E_L as a function of the distance behind the front surface of a 1-cm-thick slab of ZnSe to the linear focal position. The pulse width is 18 nsec FWHM, and the beam size at the 4-cm focal-length lens is 2.5 mm.

shown by Eq. (3), which more effectively defocus the beam; thus the fluence at some distance toward the far field will be limited. In addition, free-carrier absorption can become important. Figure 9 shows the limiting energy obtained with 18-nsec FWHM 0.53-μm pulses focused into a 1-cm-thick ZnSe slab as a function of the linear-optics focal position. The limiting energy of less than 2 μJ when the beam is focused in the bulk corresponds to a peak input power of less than 100 W. Again, the device was self-protecting in the bulk.

We have performed experiments that use picosecond pulses to give approximate scaling relations in order to optimize limiting with respect to the focusing geometry and sample thickness.[25] If the only limiting process were 2PA (e.g., as occurs in many liquid crystals[15]), the limiting energy E_L would be independent of the focusing geometry. This is true since the irradiance I is proportional to $1/w_0^2$ (w_0 is the spot radius at focus), while the effective interaction length in the sample is the depth of focus, which is proportional to w_0^2. Thus the product βIL (L is the sample length), which determines 2PA [see Eq. (1)], is independnet of the focal length. As is shown in Section 7 below, if self-defocusing is dominant even at the limiting threshold, we expect $E_L \propto w_0$. Indeed, our experiments confirm the importance of self-refraction; however, the results for the limiting energies in ZnSe using two different focal-length lenses more closely fit an even stronger dependence on spot size (nearly w_0^2).[25] Assuming that we focus as far into the sample as possible (i.e., on the back surface), we have the limiting energy independent of L but porportional to w_0. The damage energy E_D, however, depends on the beam area at the surface, which is proportional to L^2/w_0^2. This gives us a dynamic range E_D/E_L that depends on L^2/w_0^3. While the data giving this empirical scaling relation are limited, and extrapolating the results is suspect, it is clear that tight focusing (small w_0) and thick samples should give a larger dynamic range and a lower limiting threshold.

5. MONOLITHIC LIMITER

These design criteria were taken to the extreme by making the monolithic limiter shown in Fig. 2. This design takes the damage-prone surface as far from focus as is possible while maintaining high irradiance within the bulk, thus maximizing the dynamic range. The output of the frequency-doubled single-pulse mode-locked Nd:YAG laser was collimated to a spot size w_0 (half-width $1/e^2$ maximum) of 1 mm and directed into the device. Two monolithic devices were made, one of ZnSe and one of ZnS. We previously reported[25] (see Fig. 3) that the ZnSe device has a limiting energy of $\simeq$10 nJ, which corresponds to $\sim$300 W for 30-psec FWHM input 0.53-μm pulses, and a dynamic range of greater than 10^4. Optical damage to the bulk of the material is prevented by the combined effects of beam depletion due to 2PA and carrier defocusing before the focal position determined by linear optics. This monolithic limiter is thus self-protected against high-irradiance picosecond pulses. It was expected that the device would also be self-protected against nanosecond pulses, as was true when we focused less tightly into plane-parallel ZnSe samples. Unfortunately, however, both monolithic devices suffered bulk damage. When we focus extremely tightly, as in the monolithic device, the focal volume becomes so small that the temperature change due to linear and nonlinear absorption of the more energetic nanosecond pulses may give rise to a thermal nonlinearity, which in ZnSe and ZnS is a self-focusing nonlinearity. The thermal self-refraction for tight focusing may overcome the free-carrier defocusing and cause beam collapse and damage. The problem can be overcome, however, by using materials with a negative thermal nonlinearity or by not focusing so tightly. Not focusing so tightly, though, raises the limiting energy.[25]

6. BAND-GAP AND WAVELENGTH DEPENDENCE

The dimensions of the ZnSe and ZnS devices were slightly different so that, accounting for the different refractive indi-

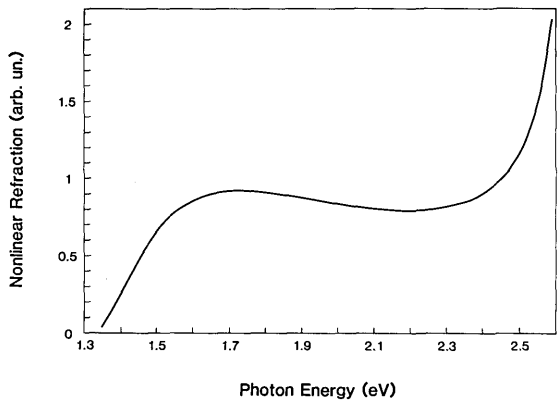

Fig. 10. Theoretical plot of the functional dependence of Δn [relation (8) in text] versus photon energy for ZnSe.

ces, the calculated (by linear optics) spot sizes in the centers of both devices were the same. The behavior of the ZnS device was qualitatively similar to that of the ZnSe device; however, the limiting energy E_L measured under similar conditions was 130 nJ, a factor of 13 higher than for ZnSe. A reason for the large difference in limiting energies is the dependence of nonlinear refraction on band-gap energy. In the model first calculated by Auston *et al.*[33] the nonlinear refractive index is given by

$$\Delta n = -\left(\frac{8\pi P^2 e^2 N}{3n(\hbar\omega)^2 E_g}\right)\frac{1}{1-(\hbar\omega/E_g)^2}, \tag{6}$$

where n is the linear refractive index, P is the Kane momentum parameter ($E_p = 2P^2m/\hbar^2$, with m the electron mass), and $\hbar\omega$ is the photon energy. From Eq. (3) the carrier density N is given by

$$N(t) = \int_{-\infty}^{t}\left(\frac{\beta I^2(t')}{2\hbar\omega}\right)dt'. \tag{7}$$

Thus N and hence Δn are proportional to $\beta/\hbar\omega$, so that by using relation (4) we obtain the frequency and band-gap dependence of the index change as

$$\Delta n \propto \frac{E_g}{(\hbar\omega)^8}\frac{(2\hbar\omega/E_g - 1)^{3/2}}{1-(\hbar\omega/E_g)^2}. \tag{8}$$

The laser frequencies are the same ($\hbar\omega = 2.34$ eV), but the energy gap for ZnSe is 2.67 eV, compared with 3.66 eV for ZnS. Therefore, for identical pulse widths and irradiances, $\Delta n(\text{ZnSe}) \simeq 8.3 \times \Delta n(\text{ZnS})$. This accounts for most of the factor-of-13 difference in measured limiting energies. As the 2PA coefficients of the materials differ by less than a factor of 3 ($\beta_{\text{ZnSe}} = 5.5$ cm/GW, $\beta_{\text{ZnS}} = 2.0$ cm/GW), we conclude that the primary limiting mechanism is the 2PA-induced free-carrier self-refraction.[27]

If we assume that the limiting begins when the overall change in phase $\Delta\Phi$ is of the order of 2π and occurs within the depth of focus $z_0 = \pi w_0^2/\lambda$, we have the change in optical path length $\Delta n z_0 \propto \lambda$ [see Eq. (2)]. For a fixed ratio $\hbar\omega/E_g$, this assumption using Eq. (7) in Eq. (6) along with $\beta \propto E_g^{-3}$ gives the limiting energy $E_L \propto I w_0^2 \propto (\hbar\omega)^{5/2} w_0$. The diffraction-limited spot radius w_0 is proportional to λ, giving the scaling relation $E_L \propto (\hbar\omega)^{3/2}$. We see immediately that we can expect much lower limiting energies at longer wavelengths when we use narrow-gap semiconductors.

Figure 10 shows the dependence of Δn [relation (8)] on the incident photon energy for ZnSe. This highlights the flat response of the limiter over almost all the range $E_g/2 < \hbar\omega < E_g$. The sharp rise in Δn from zero at $\hbar\omega = 1.33$ eV indicates the onset of 2PA at the two-photon resonance. The flat region between 1.55 and 2.4 eV (corresponding to $\lambda = 800$–500 nm) results from the slowly decreasing generation rate combined with the slowly increasing free-carrier refraction in this frequency range. As the frequency approaches the band-gap resonance, Δn rapidly increases. However, linear absorption will dominate in this region, which is undesirable for limiting. This figure clearly illustrates the broadband nature of the two-photon-induced free-carrier nonlinearity employed in these limiting devices. In what follows we show the results of a careful characterization of the output of the ZnSe monolithic limiter for picosecond input pulses in both space and time.

7. TEMPORAL AND SPATIAL RESPONSE

If we place a vidicon $\simeq 2.8$ m behind the ZnSe device (toward the far field) we see the fluence-limiting characteristics of Fig. 11. Here the temporally integrated spatial energy distribution is shown as a function of position for input energies from 13 nJ to 61 μJ. For the data shown, no filters were changed in front of the vidicon. As the input enegy is increased, the energy simply gets spread out in space, limiting the fluence and thus protecting the sensitive vidicon photocathode. If we look just at the on-axis portion of this light through a 0.4-mm aperture, we get the input–output characteristics shown in Fig. 3.

Sending the pulse through the limiter onto the entrance slit of a 2-psec-resolution streak camera allows us to look at the spatial and temporal energy distribution simultaneously on the vidicon screen. What we see at low inputs, shown in Fig. 12, is the Gaussian spatial distribution and a nearly Gaussian distribution in time. At higher input (Fig. 13), as the pulse develops, the energy spreads out in space into two wings. At still higher energies, shown in Fig. 14, the energy appears to be nearly uniformly spread in space for later times in the pulse. This is clearly advantageous from the

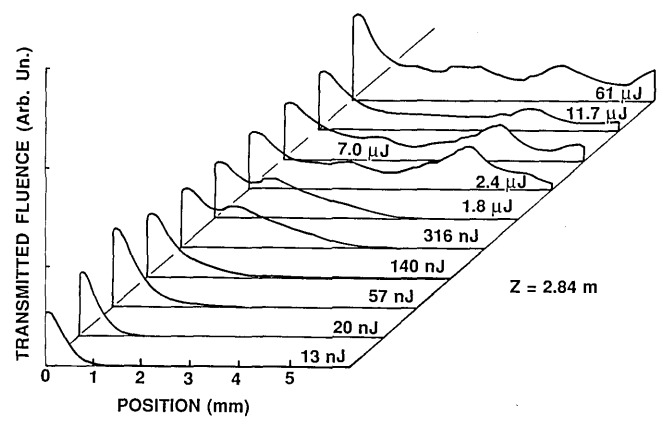

Fig. 11. Transmitted fluence at 2.8 m behind the ZnSe monolithic limiter as detected by a vidicon as a function of position at various input energies.

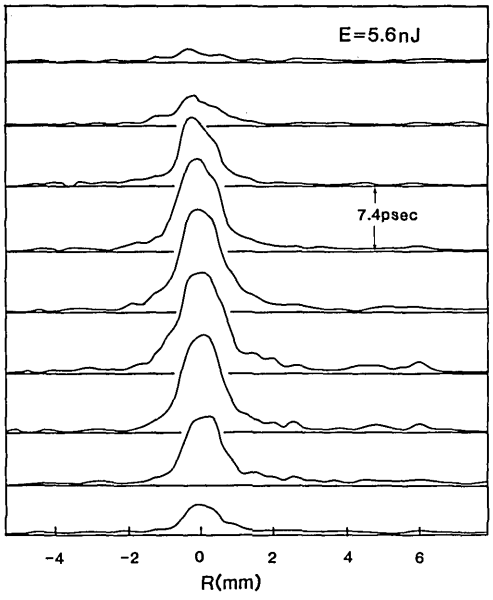

Fig. 12. Spatial energy distribution at 2.8 m behind the ZnSe monolithic limiter at various times as detected by a streak-camera–vidicon system for an input energy of 5.6 nJ.

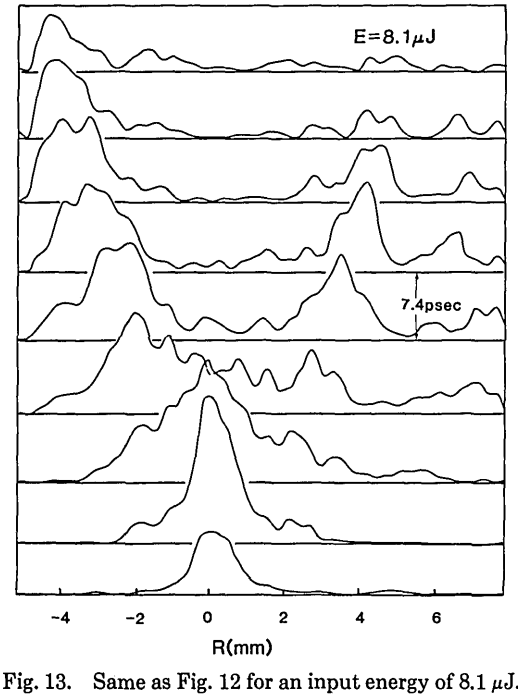

Fig. 13. Same as Fig. 12 for an input energy of 8.1 μJ.

standpoint of protecting optical components. In order to compare these results with the thin-sample results, Fig. 15 shows the spatial energy distribution at various times for a 125-μm spot radius beam traversing a 0.3-cm-thick ZnSe sample and propagating 11 cm in free space to the streak camera. While there is certainly a quantitative difference in the output, qualitatively the results are remarkably similar. This gives us confidence in using the analysis for thin samples to predict the performance of thick limiters.

Figure 16 shows the transmitted temporal structure of the output of the ZnSe monolithic limiter for a 20-μJ input pulse at various positions in the beam. The reference beam shows the position of the center of the pulse in time (i.e., when the beam is detected for low input). We see the center far advanced in time and advanced to a lesser degree as we look farther out in the beam. The original beam extended only 1 mm. What is happening is that at early times in the pulse for high input, 2PA creates free carriers, which defocus subsequent parts of the pulse. This defocusing increases with

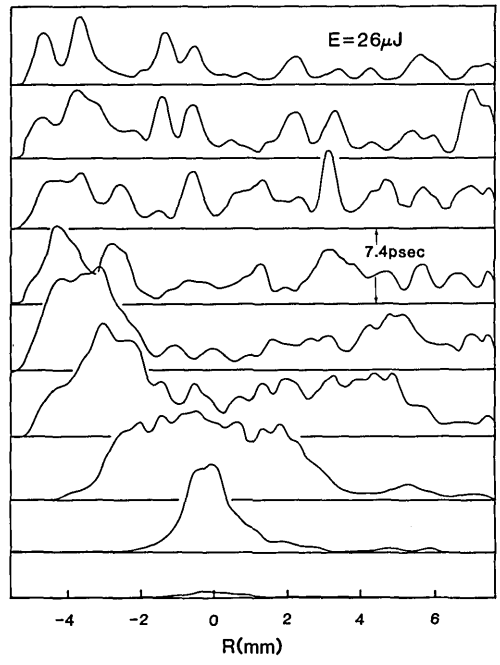

Fig. 14. Same as Fig. 12 for an input energy of 26 μJ.

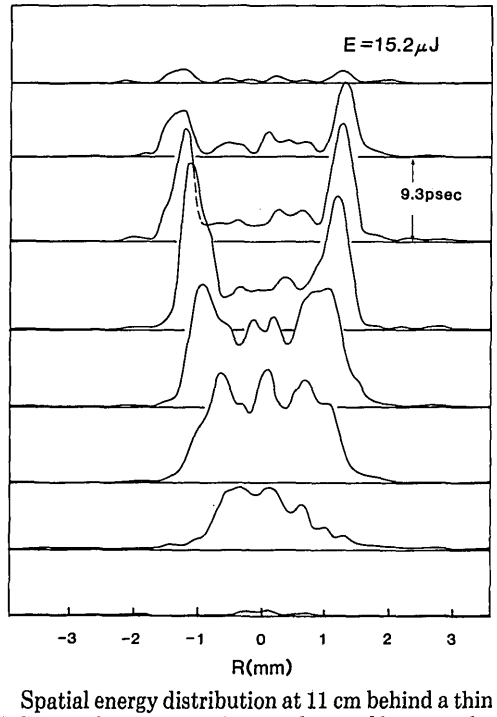

Fig. 15. Spatial energy distribution at 11 cm behind a thin (2-mm-thick) ZnSe sample at various times as detected by a streak-camera–vidicon system for an input energy of 15 μJ.

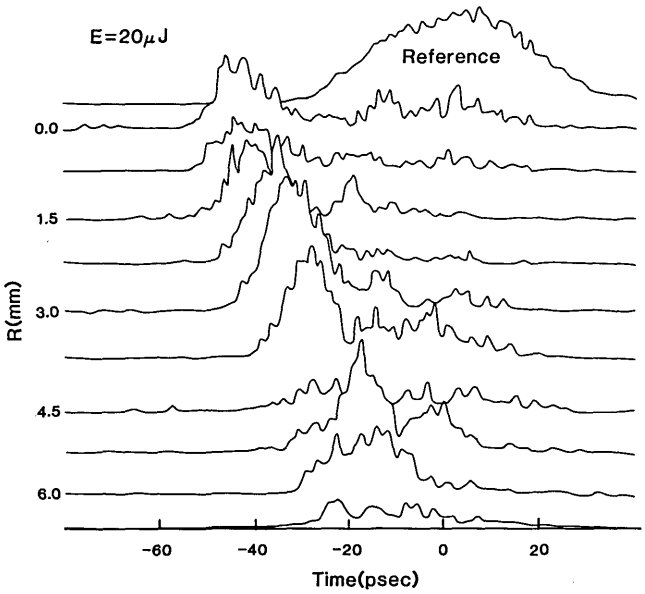

Fig. 16. Temporal energy distribution at 2.8 m behind the ZnSe monolithic limiter at various positions in the beam. A reference pulse indicating the zero time and the original pulse width is shown at the top.

time since the carrier density increases with the time integral of the square of the irradiance over time as given in Eq. (7). Therefore later portions of the beam spread out more in space, and the irradiance as well as the fluence is limited.

8. CONCLUSION

We have developed a quantitative understanding of 2PA leading to a predictive capability. That is, given n, Eg, E_p, and $\hbar\omega$, we can give the 2PA coefficient. We understand the associated defocusing as being due to the 2PA-generated free-carrier Drude–band-blocking effects. We have used a combination of these two nonlinearities to build optical limiting devices. By employing a thick limiter geometry, in which we focus tightly into the semiconductor material, we have greatly extended the dynamic range of these devices. Defocusing by two-photon-excited carriers makes these devices self-protecting. We have obtained limited energies as low as 10 nJ, which corresponds to $\simeq$300 W for the picosecond pulses used, and the dynamic range is greater than 10^4. In the case of nanosecond pulses, limiting powers below 100 W were obtained. We have determined that there are no possibly damaging hot spots in either space or time. Since 2PA is broadband, these devices are broadband (e.g., ZnSe should work from 500 to 850 nm). Also, from our study of the band-gap energy dependence of 2PA and the scaling of the resulting nonlinear refraction with wavelength, we expect that limiters using narrow-gap semiconducting material will have considerably lower limiting inputs in the infrared.

ACKNOWLEDGMENTS

We gratefully acknowledge the support of the National Science Foundation (grant ECS-8617066), and we wish to express our thanks to B. S. Wherrett for useful input during the preparation of this manuscript.

REFERENCES

1. S. A. Akhmanov, R. V. Khokhlov, and A. P. Sukhorukov, "Self-focusing, self-defocusing, and self-modulation of laser beams," in *Laser Handbook*, F. T. Arecchi and E. O. Schultz-Dubois, eds. (North-Holland, Amsterdam, 1972), Vol. 2, pp. 1151–1228.
2. E. W. Van Stryland, H. Vanherzelle, M. A. Woodall, M. J. Soileau, A. L. Smirl, S. Guha, and T. F. Boggess, "Two photon absorption, nonlinear refraction, and optical limiting in semiconductors," Opt. Eng. **24,** 613 (1985).
3. J. P. Gordon, R. C. C. Leite, R. S. Moore, S. P. S. Porto, and J. R. Whinnery, "Long-transient effects in lasers with inserted liquid samples," Bull. Am. Phys. Soc. **119,** 501 (1964).
4. J. P. Gordon, R. C. C. Leite, R. S. Moore, S. P. S. Porto, and J. R. Whinnery, "Long-transient effects in lasers with inserted liquid samples," J. Appl. Phys. **36,** 3 (1965).
5. R. C. C. Leite, R. S. Moore, and J. R. Whinnery, "Low absorption measurements by means of the thermal lens effect using a He–Ne laser," Appl. Phys. Lett. **5,** 141 (1964).
6. C. E. Rieckhoff, "Self-induced divergence of cw laser beams in liquids—a new nonlinear effect in the propagation of light," Appl. Phys. Lett. **9,** 87 (1966).
7. R. C. C. Leite, S. P. S. Porto, and P. C. Damen, "The thermal lens effect as a power limiting device," Appl. Phys. Lett. **10,** 100 (1967).
8. M. J. Soileau, "Passive intensity limiter based on nonlinear optics," J. Opt. Soc. Am. **70,** 1051 (A) (1980).
9. M. J. Soileau, W. E. Williams, and E. W. Van Stryland, "Optical power limiting with picosecond response time," IEEE J. Quantum Electron. **QE-19** 731 (1983); see also W. E. Williams, M. J. Soileau, and E. W. Van Stryland, "Optical switching and n_2 measurements in CS_2," Opt. Commun. **50,** 256 (1984).
10. E. P. Ippen and C. V. Shank "Picosecond response of a high repetition rate CS_2 optical Kerr gate," Appl. Phys. Lett. **26,** 92 (1975).
11. M. Mohebi, P. F. Aiello, G. Reali, M. J. Soileau, and E. W. Van Stryland, "Self-focusing in CS_2 at 10.6 μm," Opt. Lett. **10,** 396 (1985).
12. D. V. G. L. Narashimha Rao and S. Jayaraman, "Self-focusing of laser light in the isotropic phase of a nematic liquid crystal," Appl. Phys. Lett. **23,** 539 (1973).
13. G. K. L. Wong and Y. R. Shen, "Study of pretransitional behavior of laser-field-induced molecular alignment in isotropic nematic substances," Phys. Rev. A **10,** 1277 (1974).
14. I. C. Khoo, "Nonlinear light scattering by laser- and dc-field-induced molecular reorientations in nematic-liquid-crystal films," Phys. Rev. A **25,** 1040 (1982).
15. M. J. Soileau, S. Guha, W. E. Williams, E. W. Van Stryland, H. Vanherzeele, J. L. W. Pohlmann, E. J. Sharp, and G. Wood, "Studies of the nonlinear switching properties of liquid crystals with picosecond pulses," Mol. Cryst. Liq. Cryst. **127,** 321 (1985).
16. J. E. Bjorkholm, P. W. Smith, W. J. Tomlinson, and A. E. Kaplan, "Optical bistability based on self-focusing," Opt. Lett. **6,** 345 (1981); also J. E. Bjorkholm, P. W. Smith, and W. J. Tomlinson, "Optical bistability based on self-focusing: an approximate analysis," IEEE J. Quantum Electron. **QE-18,** 2016 (1982).
17. D. A. B. Miller, C. T. Seaton, M. E. Prise, and S. D. Smith, "Bandgap-resonant nonlinear refraction in III–V semiconductors," Phys. Rev. Lett. **47,** 197 (1981).
18. J. E. Geusic, S. Singh, D. W. Tipping, and T. C. Rich, "Three photon stepwise optical limiting in silicon," Phys. Rev. Lett. **19,** 1126 (1969).
19. T. F. Boggess, S. C. Moss, I. W. Boyd, and A. L. Smirl, "Nonlinear-optical energy regulation by nonlinear refraction and absorption in silicon," Opt. Lett. **9,** 291 (1984).
20. J. M. Ralston and K. R. Chang, "Optical limiting in semiconductors," Appl. Phys. Lett. **15,** 164 (1969).
21. A. C. Walker, A. K. Kar, Wei Ji, U. Keller, and S. D. Smith, "All-

optical power limiting of CO_2 laser pulses using cascaded optical bistable elements," Appl. Phys. Lett. **48,** 683 (1986).
22. A. K. Kar, J. G. H. Mathew, S. D. Smith, B. Davis, and W. Prettl, "Optical bistability in InSb at room temperature with two photon excitation," Appl. Phys. Lett. **42,** 334 (1983).
23. T. F. Boggess, A. L. Smirl, S. C. Moss, I. W. Boyd, and E. W. Van Stryland, "Optical limiting in GaAs," IEEE J. Quantum Electron. **QE-21,** 488 (1985).
24. D. J. Hagan, E. W. Van Stryland, M. J. Soileau, and Y. Y. Wu, "Semiconductor optical limiters with large dynamic range," J. Opt. Soc. Am. A **3**(13), P105 (1986).
25. D. J. Hagan, E. W. Van Stryland, M. J. Soileau, and Y. Y. Wu, "Self-protecting semiconductor optical limiters," Opt. Lett. **13,** 315 (1988).
26. V. S. Butylkin, A. E. Kaplan, and Yu. G. Kronopulo, "Possibility of observing self-focusing due to the stimulated Raman effect," Radiophys. Quantum Electron. **12,** 692 (1969).
27. E. W. Van Stryland, M. A. Woodall, H. Vanherzeele, and M. J. Soileau, "Energy band-gap dependence of two-photon absorption," Opt. Lett. **10,** 490 (1985).
28. P. Liu, W. L. Smith, H. Lotem, J. H. Bechtel, and N. Bloembergen, "Absolute two-photon absorption coefficients at 355 and 266 nm," Phys. Rev. B **17,** 4620 (1978).
29. J. Dempsey, J. Smith, G. D. Holah, and A. Miller, "Nonlinear absorption and pulse-shaping in InSb," Opt. Commun. **26,** 265 (1978); A. M. Johnson, C. R. Pidgeon, and J. Dempsey, "Frequency dependence of two-photon absorption in InSb and HgCdTe," Phys. Rev. B **22,** 825 (1980); C. R. Pidgeon, B. S. Wherrett, A. M. Johnston, J. Dempsey, and A. Miller, "Two photon absorption in zinc-blende semiconductors," Phys. Rev. Lett. **42,** 1785 (1979).
30. S. Guha, E. W. Van Stryland, and M. J. Soileau, "Self-defocusing in CdSe induced by charge carriers created by two-photon absorption," Opt. Lett. **10,** 285 (1985).
31. J. A. Hermann, "Beam propagation and optical power limiting with nonlinear media," J. Opt. Soc. Am. B **1,** 729 (1984).
32. J. A. Hermann, "Simple model for a passive optical power limiter," Opt. Acta **32,** 541 (1985).
33. D. H. Auston, S. McAffee, C. V. Shank, E. P. Ippen, and O. Teschke, "Picosecond spectroscopy of semiconductors," Solid State Electron. **21,** 147 (1978).

E. W. Van Stryland

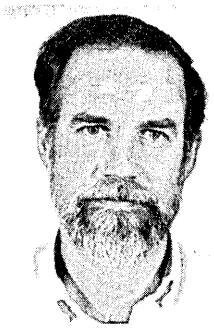

E. W. Van Stryland was born on June 3, 1947. He received the Ph.D. degree in physics in 1976 from the University of Arizona, Tucson, where he worked at the Optical Sciences Center on optical coherent transients. He worked in the areas of femtosecond pulse production, multiphoton absorption in solids, and laser-induced damage at the Center for Laser Studies at the University of Southern California, Los Angeles. He joined the physics department at North Texas State University in 1978 and was instrumental in forming the Center for Applied Quantum Electronics there. In 1987 he joined the newly formed Center for Research in Electro-Optics and Lasers at the University of Central Florida, Orlando, where he is a professor of physics and electrical engineering working in the area of nonlinear optics.

Y. Y. Wu

Y. Y. Wu was born in Beijing, China, on June 21, 1954. She received the M.S. degree in electrical engineering in 1982 from Chengdu Institute of Radio Engineering, China. She obtained the M.S. degree in physics in 1984 from North Texas State University, Denton, Texas, where she worked as a Ph.D. candidate at the Center for Applied Quantum Electronics. Currently she is continuing her Ph.D. project in characterizing the nonlinear optical properties of semiconductors at the Center for Research in Electro-Optics and Lasers with the University of Central Florida.

D. J. Hagan

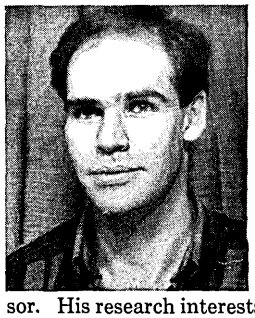

D. J. Hagan was born in Edinburgh, Scotland, in 1959. He received the B.S. and Ph.D. degrees from Heriot-Watt University in 1982 and 1985, respectively. After working for two years as a research scientist in the Center for Applied Quantum Electronics at North Texas State University, he moved to the Center for Research in Electro-Optics and Lasers at the University of Central Florida, where he is currently an assistant professor. His research interests include four-wave mixing, optical bistability, optical power limiting, and optical nonlinearities in bulk and microcrystalline semiconductors. Dr. Hagan is a member of the Optical Society of America, the Society of Photo-Optical Instrumentation Engineers, and the Institute of Electrical and Electronics Engineers.

M. J. Soileau

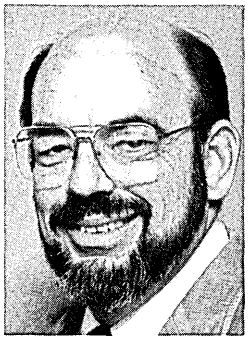

M. J. Soileau was born on June 27, 1944. He received the Ph.D. degree in quantum electronics in 1979 from the University of Southern California, Los Angeles, where he worked at the Center for Laser Studies on laser-induced damage to wide-band-gap optical materials. He spent six years in the U.S. Air Force and worked for seven years at the Navy Michelson Laboratory. He joined the faculty of the Department of Physics of North Texas State University in 1980 and was a founding member of the Center for Applied Quantum Electronics. In 1987 he became the first director of the newly formed Center for Research in Electro-Optics and Lasers at the University of Central Florida, where he is a professor of electrical engineering and physics. His research interests include laser-induced damage to optical materials, nonlinear absorption and refraction, and optical limiting.